

---

# Scan-point Planning and 3-D Map Building for a 3-D Laser Range Scanner in an Outdoor Environment

Keiji NAGATANI<sup>1</sup>, Takayuki Matsuzawa<sup>1</sup>, and Kazuya Yoshida<sup>1</sup>

Tohoku University

**Summary.** During search missions in disaster environments, an important task for mobile robots is map building. An advantage of three-dimensional (3-D) mapping is that it can provide depictions of disaster environments that will support robotic teleoperations used in locating victims and aid rescue crews in strategizing. However, the 3-D scanning of an environment is time-consuming because a 3-D scanning procedure itself takes a time and scan data must be matched at several locations. Therefore, in this paper, we propose a scan-point planning algorithm to obtain a large scale 3-D map, and we apply a scan-matching method to improve the accuracy of the map. We discuss the use of scan-point planning to maintain the resolution of sensor data and to minimize occlusion areas. The scan-matching method is based on a combination of the Iterative Closest Point (ICP) algorithm and the Normal Distribution Transform (NDT) algorithm. We performed several experiments to verify the validity of our approach.

**Key words:** Search and Rescue, Scan points planning

## 1 Introduction

Recently, requests for the development of robotic systems for search-and-rescue operations have been increasing rapidly. After the Hanshin-Awaji earthquake in 1995 (Japan) and the World Trade Center attack in 2001 (U.S.A.), large research projects for search and rescue were kicked off in Japan.

One of the important tasks for mobile robots in search-and-rescue missions is map building. Three-dimensional (3-D) mapping is used to provide representations of disaster environments that will support robotic teleoperations used in locating victims and aid rescue crews in strategizing. To realize 3-D mapping in disaster environments, we constructed the 3-D scanner device shown in Figure 1-(a). It consists of a laser range finder (SICK), rotation stage, and CCD camera to obtain information in color. It takes one minute to scan an environment at one place, and the device generates 3-D information to create a remote display of the target environment (e.g., Figure 1-(b)), which helps the rescuers get a complete picture.

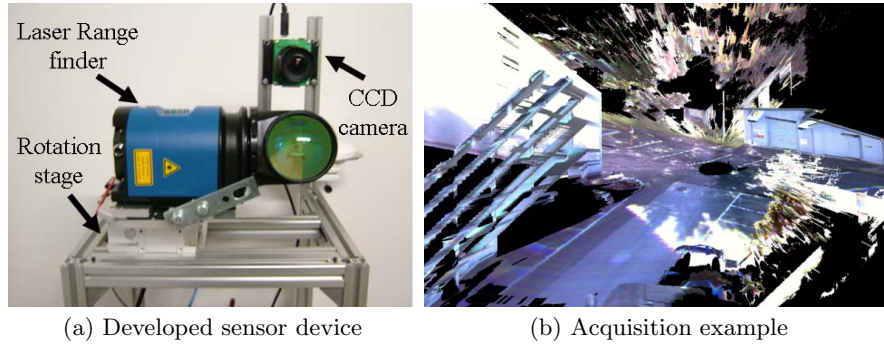


**Fig. 1.** Development of a sensor system and acquisition example of an environment

Search-and-rescue missions require rapid, accurate mapping. However, to map a large-scale environment, rescue robots must obtain 3-D information in different locations, and the scan data obtained at different locations should be merged to represent a large-scale environment. In such cases, reasonable scan-point planning is very important; however, measurements in different locations generate gaps of objects in the map caused by positioning errors at each scan point. Therefore, we propose a scan-point planning algorithm to obtain a large scale 3-D map, and we have applied a scan-matching method to improve map accuracy. In the scan-point planning algorithm, the resolution of sensor data and occlusion area allow as much of a target area as possible to be covered. The scan-matching method is based on the Iterative Closest Point (ICP) algorithm [1] and the Normal Distribution Transform (NDT) algorithm [2]. In this paper, we discuss the construction of 3-D maps in outdoor environments, and we report the results of the environment mapping of our campus buildings.

## 2 Related Works

Two major approaches are used to obtain a 3-D map. One, stereo matching, involves the use of two or more cameras (e.g., [3]), while the other involves a 3-D laser range scanner (e.g., [4]). The merits of the former approach are fast measurement and simultaneous acquisition of texture information. However, there are some disadvantages: (1) stereo matching requires brightness and feature information, (2) its measurement area is narrow, and (3) distance accuracy decreases as the distance from the objects increases. Therefore, in this study, we use a 3-D laser range scanner with a CCD camera to produce the 3-D color map shown in Figure 1.

In regard to scan-point planning, a classic problem is the Art Gallery Problem [5], which involves the number of guards required to monitor the target floor completely. Basically, the problem assumes that the shape of the floor is known and the target environment is 2-dimensional (2-D). Recently, some novel researches for view point planning were performed in 3-D. Sequeira et

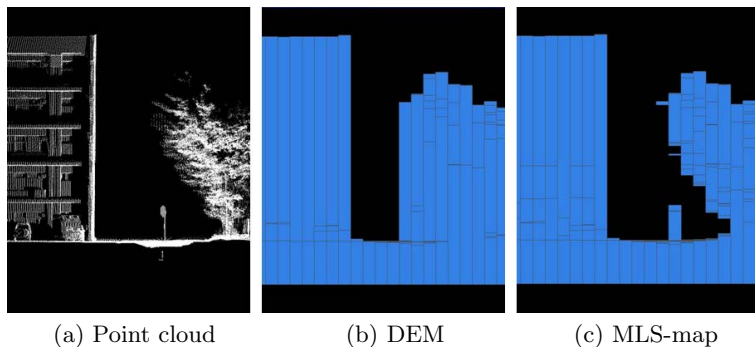


**Fig. 2.** Comparison of DEM and MLS-map

al. proposed a view planning method for automatic acquisition of environment information with consideration of sampling density [6]. In our scan-point planning, we propose a scan-point planning method that combines frontier-based navigation [7] and the Art Gallery Problem.

Recently, scan matching has been used for the adjustment of the relative position of the scan data and particularly for simultaneous localization and mapping (SLAM) in mobile robot navigation[8]. In this research, we apply the conventional Iterative Closest Points (ICP) algorithm [1] and the Normal Distribution Transform (NDT) algorithm [2] to our scan data. Because both algorithm have advantages and disadvantages, we have combined them to obtain a robust and accurate 3-D map.

### 3 Scan-Point Planning

To obtain a large scale environment by repeated 3-D scanning, we have established the following procedures:

1. Conducting a 3-D scan
2. Representing the scan information on a Multi-Level Surface map (MLS-map)
3. Determining the movable region
4. Planning the next scan point in the region
5. Moving the 3-D scanner to the designated point
6. Repeating steps 1 through 5 until the target region is completely covered

#### 3.1 Representation of scan information

To perform scan-point planning in large-scale environments, point cloud representation is unsuitable because of the massive volume of data and the non-constant density. Therefore, at the beginning of this study, we applied a Digital Elevation Map (DEM) to represent target environments [9] for scan-point

planning. In this method, each scan point is registered into one cell of the lattice domain on a 2 dimensional (2-D) x-y plane as height information from a base level. The DEM advantageously represents a non-flat environment. However, the method can not be used to represent spaces under objects because only the highest scan point is effective. An example of point cloud representation is shown in Figure 2-(a). It is a side view of a four-story building (left) and a tree (right). A DEM representation of Figure 2-(a) is shown in Figure 2-(b) from the same viewpoint. A space under the tree is not visible in the DEM representation, which is undesirable for the determination of the movable region of mobile robots.

A Multi-Level Surface map (MLS-map) [10] is one solution to the representation of such an environment. In this method, some edge-point positions of objects are stored in each cell of the lattice domain on a 2-D x-y plane. Figure 3 shows a concept of the MLS-map. Information about two objects is stored in one cell, which represents a space between the objects. Based on the above method, the point cloud representation in Figure 2-(a) is represented by the MLS-map in Figure 2-(c). The space under the tree is now visible.

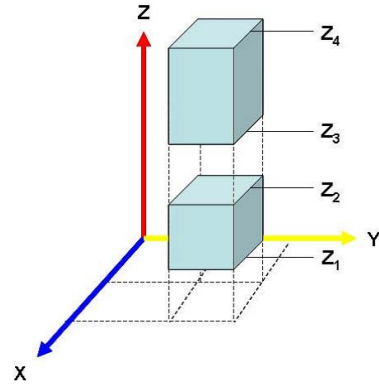


Fig. 3. Introduction to MLS map

### 3.2 Determination of movable region

For mobile robots, the path between the current scan point and the next scan point must be connected. Therefore, we define a movable region as an area (1) which is connected to a current scan point and (2) whose differential height between adjacent cells in the MLS-map is smaller than the threshold. Of course, the movable region depends on the mobility of the target mobile robot. In our implementation, the threshold was set at 0.15 [m].

### 3.3 Region segmentation

To maintain the resolution of scan data, we divide the target region into three regions, (1) scan-completed region, (2) low-resolution region, and (3) unscanned region. In reality, map resolution depends on not only the scan range but also the orientation; however, to simplify the planning of the next scan points, we use the following definitions: (1) The scan-completed region ( $C$ ) is a set of cells in the target region which has scan data and whose distance from the closest scan point is less than a fixed value. In our implementation, the distance value is set at 20 [m]. (2) The low-resolution region ( $M$ ) is a set of cells in the target region which has scan data but does not belong to the scan-completed region. (3) The unscanned region ( $U$ ) is a region which does

not belong to (1) and (2) because a cell in the region is too far from the scan points or is occluded by objects.

Figure 4 shows an example of the region segmentation of an initial scan from scan point  $A$ . The white region is the scan-completed region ( $C_A$ ) from point  $A$ , the gray region is the low-resolution region ( $M_A$ ), and the blue rectangles are obstacles. The dark-gray region is the unscanned region ( $U$ ), where the blue rectangles occlude or are far from point  $A$ .

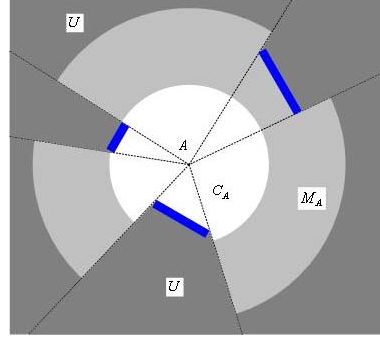


Fig. 4. Region segmentation

### 3.4 Evaluation function for next scan point

To minimize the scan procedure while maintaining the resolution of the scan data, the unscanned region or the low-resolution region should be changed, as much as possible, into a scan-completed region by the next scan. Two different indices are included, therefore, we defined an evaluation function as follows:

$$F_X = \text{area}((U \cap C_B) \cup (U \cap M_B)) \cdot \alpha + \text{area}(M_A \cap C_B) \cdot (1 - \alpha) \quad (1)$$

where  $\text{area}(\cdot)$  is an area value in the bracket,  $C_B$  is a prospective area which becomes a scan-completed region when the next scan is conducted at point B,  $M_B$  is a prospective area which becomes a low-resolution region when the next scan is conducted at point B, and  $\alpha$  is the weight value. If exploration in the unscanned region is not important, the  $\alpha$  should be very small or zero.

The calculation of Equation (1) at one cell in the movable region requires a ray-tracing scan in 3-D virtual space, which is time-consuming. Therefore, we applied a hill-climbing search from several randomized initial locations.

Figure 5 shows a top view of an example of a planned result in an MLS-map in the case of an initial scan. In this figure, the blue circle depicts an initial scan point, the red circle is the planned scan point in the case of  $\alpha = 1.0$ , the green circle is the planned scan point in the case of  $\alpha = 0.0$ , the flesh-colored region is the scan-completed area, the yellow region is a low-resolution movable area, and the blue region is a low-resolution but not movable area. Figure 6 shows virtual views, (a) is a view from the initial scan point corresponding to the blue circle in Figure 5, (b) is a view from the planned scan point in the case of  $\alpha = 0.0$  corresponding to the red circle in Figure 5, and (c) is a view from the planned scan point in the case of  $\alpha = 1.0$  corresponding to the green circle in Figure 5. In the virtual views, scanning in unknown area has priority in the case of  $\alpha = 1.0$ .

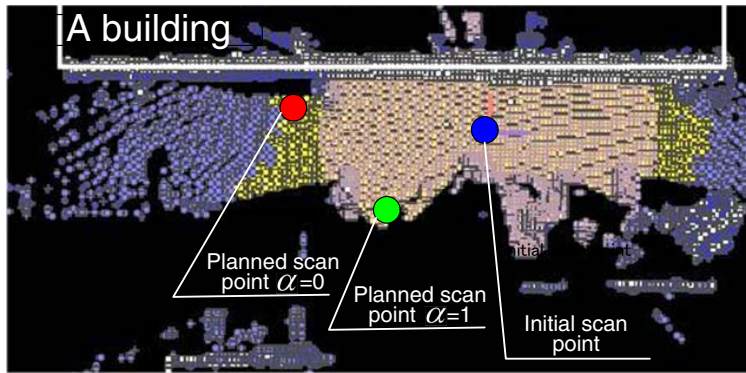
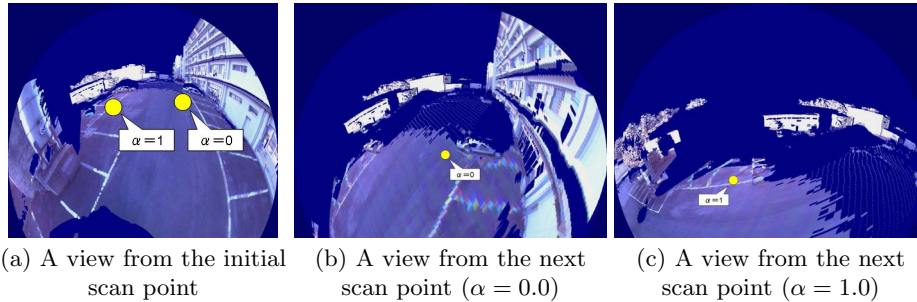


Fig. 5. Top view of an example of target region



(a) A view from the initial scan point (b) A view from the next scan point ( $\alpha = 0.0$ ) (c) A view from the next scan point ( $\alpha = 1.0$ )

Fig. 6. An example of a scan point

### 3.5 Examples of planning results in outdoor environments

We tried the above scan-point planning method in several different outdoor environments. The motion of the 3-D scan unit to the next scan position was performed by a human operator, not by a mobile robot platform. Termination judgement was made by the operator, who checked the coverage region. Due to space limitations, only one experimental result will be discussed here.

The target environment is our campus (Mechanical Department, Aoba-Yama, Tohoku University, Japan), which includes buildings, trees, and parking slots. The weighting factor of  $\alpha$  is set at 0.5, and the cell size of the MLS-map is set at 1.0 [m] square. Figure 7 shows a transition of the scan position and scan area in the first environment. In the 13 scan and movement motions, the detection area (the map itself) was expanded step by step. The total detection area is about 16,500 grids (that is equal to square meters). The result shows that our proposed algorithm worked well for the large-scale outdoor environment.

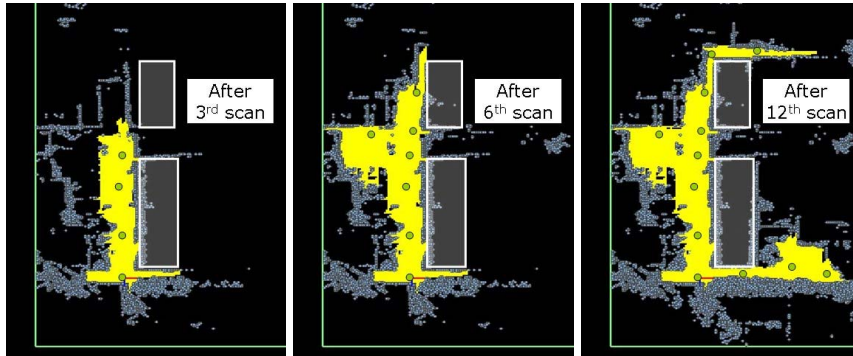


Fig. 7. A result of scan-point planning in an outdoor environment (our campus)

#### 4 Scan matching for improved map accuracy

In outdoor environments, global positioning systems (GPS), electromagnetic sensors, and inclination sensors can be used to obtain a scan point. However, because of sensing errors or noise, each scan-point location may include a positioning error. To compensate for such errors, scan matching is used to adjust the location and to construct an accurate map, particularly in simultaneous localization and mapping (SLAM). For scan matching, we apply the Iterative Closest Point (ICP) algorithm [1] and the Normal Distribution Transform (NDT) algorithm [2].

##### 4.1 Summary of the ICP algorithm

In the ICP algorithm, two given point sets are registered in Cartesian coordinates. In each iteration step, the algorithm selects the closest points as correspondences and calculates the rotation matrix  $\mathbf{R}$  and the translation matrix  $\mathbf{t}$  to minimize the following equation:

$$E(\mathbf{R}, \mathbf{t}) = \sum_{i=1}^{N_m} \sum_{j=1}^{N_d} \omega_{i,j} \|\mathbf{m}_i - (\mathbf{R}\mathbf{d}_j + \mathbf{t})\|^2 \quad (2)$$

where  $N_m$  and  $N_d$  are the number of points in the reference data set  $M$  and the matching data set  $D$  respectively.  $\omega_{i,j} = 1$  when  $\mathbf{m}_i$  is the closest point to  $\mathbf{d}_j$ , and  $\omega_{i,j} = 0$  otherwise.

To improve the accuracy of the ICP algorithm, we applied the ICP algorithm of points and segments, which calculates, not a distance between the closest points, but a distance between a point in the reference data set and a segment between two closest points in the matching data set. We call this algorithm a line-segment ICP algorithm.

## 4.2 Summary of the NDT algorithm

In the NDT algorithm, a target space is divided into grids. Then the distribution of scan points in the reference data set in one grid is represented by a normal distribution. An average in the grid  $i$  is represented by  $\mathbf{q}_i$ , and a covariance matrix in the grid is represented by  $\boldsymbol{\Sigma}_i$ . Based on the above data, an evaluation function is defined as the sum of the matching level between a point  $\mathbf{x}'_i$  in the matching data set and the normal distribution  $i$ , which corresponds to point  $\mathbf{x}'_i$ , as follows:

$$E(p) = \sum_i^{N-1} \exp \frac{-(\mathbf{x}'_i - \mathbf{q}_i)^t \boldsymbol{\Sigma}_i^{-1} (\mathbf{x}'_i - \mathbf{q}_i)}{2} \quad (3)$$

Detailed explanations and equations are given in [2].

The accuracy of the result depends greatly on the size of each grid. To improve the robustness of the NDT algorithm, we applied an algorithm in which the size of each grid is dynamically changed. At first, grid size is large for global matching. After that, the matching sequence is repeated with progressively smaller grid sizes. In our implementation, the initial size of the grid is 20 [m], the second size is 15 [m], and the final size is 10 [m]. We call this algorithm the Narrower NDT algorithm.

## 4.3 Combination of the ICP and NDT algorithms

To construct an accurate 3-D map of an outdoor environment, we applied the above scan-matching algorithms to our experimental results, as shown in section 3.5. We mounted an inclination sensor on the 3-D scanner, so the adjustment parameters in this scan matching are the position  $(x, y, z)$  and orientation  $\theta$  of an obtained environment.

Through the above application experience, we identified the following comparative qualitative features: (1) The ICP algorithm is more accurate than the NDT algorithm when the matching is successful. (2) The ICP algorithm becomes stuck in the local minima much more easily than the NDT algorithm does. Based on the above features, to pursue both accuracy and robustness for scan matching, we propose a combination of the two algorithms, or the NDT-ICP Combination. First, the Narrower NDT algorithm is applied, and then the line-segment ICP algorithm is applied.

Figure 8 shows a graph comparing the above three matching algorithms (left) and scan locations (right). Table 1 shows the numerical evaluation values of the same result. A “number-number” represents the scan location indices for matching; for example, “2-3” represents a match between scan point 2 and scan point 3. Each evaluation value is the ICP score calculated by Equation 2. The smaller of the evaluation values denotes better matching.

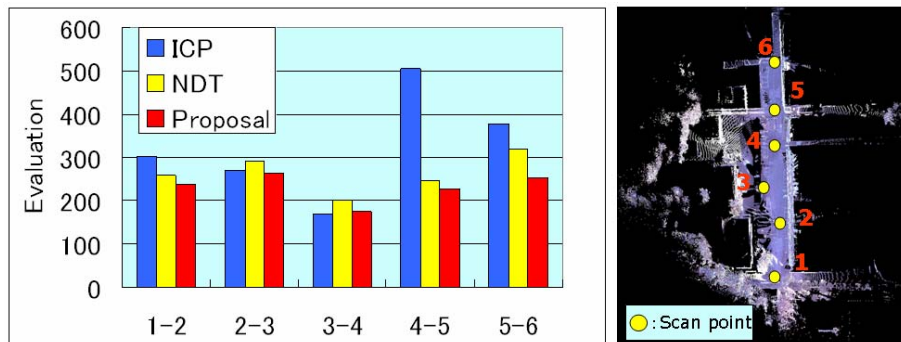


Fig. 8. A comparison of matching algorithms (our campus)

Based on the comparison results, the NDT-ICP Combination algorithm works well. In the case of scan matching between scan points 4 and 5, the solo ICP algorithm failed to match. The failed example is shown in detail in Figure 9. White dots are scan data obtained at scan point 4, and green dots are those obtained at scan point 5, where the scan points of path 1 appeared. The scan data of path 2, obtained at scan point 4, disappeared. However, the scan data of path 1 seemed to be pulled by the scan data of path 2. Finally, matching failed, as shown in the figure. In the case of the NDT-ICP Combination algorithm, such mismatching did not happen. In the case of scan matching between scan points 3 and 4, the ICP algorithm was slightly better than the NDT-ICP Combination algorithm, perhaps because the convergence direction of the solo ICP algorithm was different from the direction after the NDT algorithm was applied and the ICP iteration was stopped in the different situations.

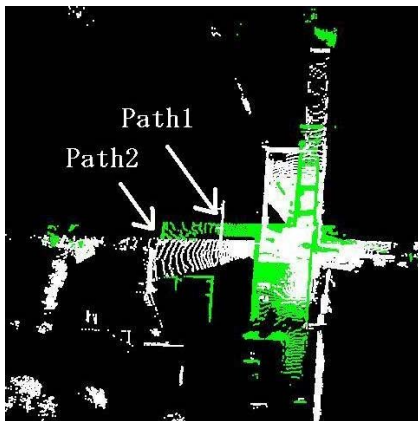


Fig. 9. Matching result “4-5” by solo ICP algorithm

Table 1. Scan Matching Comparison : Proposal

	1-2	2-3	3-4	4-5	5-6
Line-segment ICP	301.0	269.2	169.2	503.9	378.4
Narrower NDT	258.7	292.1	201.9	245.6	317.7
Proposal (NDT-ICP Comb.)	236.1	262.7	173.9	226.5	254.3

## 5 Conclusions and future work

In this paper, we have proposed a scan-point planning algorithm to obtain a large scale 3-D map efficiently and a combination of scan-matching algorithms (NDT and ICP) to improve mapping accuracy. Finally, we have offered an example of mapping in an outdoor environment to confirm the validity of the above approach. We have also applied the approach to two different environments, a small natural field at Mt. Aosasa in Sendai City and a park on our campus (without large buildings). In both environments, the proposed approach worked well. In the former case, the target environment included small trees, and the solo ICP algorithm became stuck in the local minima for scan matching. These results are not included here due to space limitations.

In our current implementation of scan-point planning, we have not considered the moving cost of mobile robots. Therefore, the next scan point may be far from the current scan point, as happened in the planning procedure shown in this paper. In the future works, it is required to discuss optimality of the viewpoint selection deeply. Furthermore, although we have defined scan resolution simply as the distance to an object, it should be considered in the orientation of the targets. By solving the above problems, we aim to obtain a feasible and accurate 3-D map in an outdoor environment.

## References

1. Paul J. Besl and Neil D. McKay. A method for registration of 3-d shapes. *IEEE Tran. on Pattern Analysis and Machine Intelligence*, 14(2):239–256, 1992.
2. Peter Biber and Wolfgang Straber. The normal distributions transform: A new approach to laser scan matching. In *IEEE/RSJ International Conference on Intelligent Robots and Systems*, pages 2743–2748, 2003.
3. Nicholas Ayache. *Artificial Vision for Mobile Robots*. MIT Press, 1991.
4. K Ikeuchi and Y Sato. *Modeling from Reality*. Kluwer Academic Publishers, 2001.
5. Joseph O’ Rourke. *Art Gallery Theorems and Algorithms*. Oxford University Press, 1987.
6. Konrad Klein and Vitor Sequeira. View planning for the 3d modelling of real world scenes. In *Proc. of IEEE/RSJ International Conference on Intelligent Robots and Systems*, 2000.
7. B. Yamauchi. A frontier-based approach for autonomous exploration. In *IEEE International Symposium on Computational Intelligence in Robotics and Automation*, pages 146–151, 1997.
8. Sebastian Thrun, Wolfram Burgard, and Dieter Fox. *Probabilistic Robotics*. The MIT Press, 2005.
9. E.H.L. Fong, W. Adams, F. L. Crabbe, and A. C. Schultz. Representing a 3-d environment with a 2 1/2-d map structure. In *IEEE/RSJ Conference on Intelligent Robots and Systems*, pages 2986–2991, 2003.
10. Rudolph Triebel, Patrick Pfaff, and Wolfram Burgard. Multi-level surface maps for outdoor terrain mapping and loop closing. In *IEEE/RSJ International Conference on Intelligent Robots and Systems*, pages 2276–2282, 2006.